Differential-Mode Vibrational Noise Cancellation Structure for Metglas/Pb(Zr,Ti)O_3 Fiber Magnetoelectric Laminates

Junqi Gao, Junyi Zhai, Ying Shen, Liangguo Shen, David Gray, Jiefang Li, Peter Finkel, and D. Viehland

***Abstract*—A differential structure which has the ability to reject external vibrational noise for Metglas/Pb(Zr,Ti)O_3 (PZT) fiber-based magnetoelectric (ME) heterostructures has been studied. This type of ME structure functions better than conventional sensors as a magnetic sensor when used in an environment in which vibrational isolation is impractical. Sensors fabricated with this differential mode structure can attenuate external vibrational noise by about 10 to 20 dB at different frequencies, while simultaneously having a doubled ME voltage coefficient. Interestingly, in addition to offering a means of mitigating vibrational noise, this ME structure offers the potential to be a hybrid sensor, separating magnetic and acoustical signals.**

I. Introduction

Magneto-electric (ME) materials, which are capable of exhibiting a change in electric polarization under magnetic field or a change in magnetization with applied electric field [1], have been the subject of recent research interest because of their potential for sensor, data storage, and communication applications [2]. The ME effect was first observed about 50 years ago in Cr_2O_3 single crystals, albeit with a small ME voltage coefficient of $\alpha_{ME} \approx 20$ mV/cm·Oe [3]. To date, single-phase materials with strong ME coupling effects have not been found. Instead, research has focused on the development of engineered ME multi-phase systems [4]–[6].

The engineered ME structures that have high ME responses are two-phase composites consisting of magnetostrictive and piezoelectric phases [7], [8]. Neither phase displays magnetoelectric properties individually. However, they can achieve ME coupling through a magneto-elasto-electric interaction [7]. The ME coupling coefficients for such multi-phase composites have much larger values than those of single-phase materials. For example, long-type sandwiched laminate structures comprised of Metglas (Vitrovac Inc., Hannau, Germany) and Pb(Zr,Ti)O_3 (PZT) fiber layers can have α_{ME} values of up to 22 V/cm·Oe [9]. Such high ME coefficients offer the potential for a new class of magnetic field sensors that are highly sensitive, passive, and capable of room-temperature operation.

There are, however, potential problems that limit the sensitivity of ME sensors. The biggest challenge for ME sensors is to reduce the equivalent magnetic noise floor, which is affected by environmental or external noise sources. Thermal fluctuation coupled into the noise via the pyroelectric effect and mechanical vibrations coupled via the piezoelectric effect [10] pose significant obstacles to practical application of ME sensors. There have been several studies concerned with external noise rejection. For example, a symmetric Terfenol-D/PZT bimorph laminated structure has been developed to reject thermal fluctuation noise [10]. Similarly, symmetric signal/unsymmetrical noise (SS-UN) and unsymmetrical signal/symmetric noise (US-SN) modes have been developed for Terfenol-D/PZT ME laminates with the capability of thermal noise rejection [11]. However, vibrational noise rejection has proven more difficult for ME laminates. This may be due, in part, to an inability of accelerometers placed in the vicinity of ME laminates to cancel vibrational noise in the laminates.

In this paper, we report a differential structure for Metglas/PZT laminates. Using this structure, vibrational signals can be reduced by a factor of 10 to 20 dB, whereas the response to applied magnetic fields is doubled relative to prior non-differential ME laminate sensors. Such vibrational noise rejection capabilities offer practical use of Metglas/PZT laminates for device applications.

II. Experimental Techniques

Fig. 1(a) illustrates our new laminate structure design for vibrational noise cancellation. Unlike other Metglas/PZT/Metglas sandwich structures, two layers of PZT were used to create a differential symmetric structure. The PZT fibers were fabricated by dicing 170-µm PZT wafers (Smart Materials, Sarasota, FL) into 40 mm long × 2 mm wide fibers. Five such PZT fibers were oriented along the longitudinal axis to form composite PZT layers 10 mm wide and 40 mm long. Two such PZT layers were fabricated, and epoxied to either side of a double-sided interdigitated Kapton-based electrode (Kapton, DuPont, Wilmington, DE). The copper traces on the electrode were 150 µm wide and were spaced 1 mm from center to center. A single-sided electrode with identical geometry was then

Manuscript received February 3, 2011; accepted June 3, 2011. The authors would like to thank DARPA and ONR for support of this work.

J. Gao, J. Zhai, Y. Shen, L. Shen, D. Gray, J. Li and D. Viehland are with the Department of Materials Science and Engineering, Virginia Tech, Blacksburg, VA (e-mail: junqi08@vt.edu).

P. Finkel is with the Naval Undersea Warfare Center, Newport, RI.

Digital Object Identifier 10.1109/TUFFC.2011.1980

bonded bare to the top and bottom surfaces of the PZT layers in a multi-push-pull geometry. The PZT composite was then poled under 2 kV/mm for 15 min at room temperature. Metglas foils (Vitrovac Inc., Hanau, Germany) which have saturation magnetostriction of 42 ppm were cut to 10 mm width and 80 mm length. Three Metglas foils were then laminated to both the top and bottom of the dual PZT laminate core to provide an optimal volume ratio between the piezoelectric and magnetostrictive phases [12].

Fig. 1(b) shows the poling configuration of the structure. In our design, the two PZT fiber layers were poled along the same orientation. Because of the symmetrical nature of the structure, the double-sided electrode in the middle acts as a neutral plane. Application of a magnetic field along the longitudinal direction of the laminate will cause the sensor to contract or elongate longitudinally. Contraction or expansion in the plane of the sensor will result in an identical charge in each PZT layer. Parallel electrical connection of the PZT layers would therefore result in a doubling of the signal. Conversely, an applied external vibrational signal will tend to cause an asymmetric (bending mode) deformation [see inset of Fig. 1(b)]. Simultaneous elongation of the top PZT and contraction of the bottom PZT will result in charges of opposite polarity in the PZT layers. Parallel electrical connection of the PZT, therefore, results in an attenuation of the output signal.

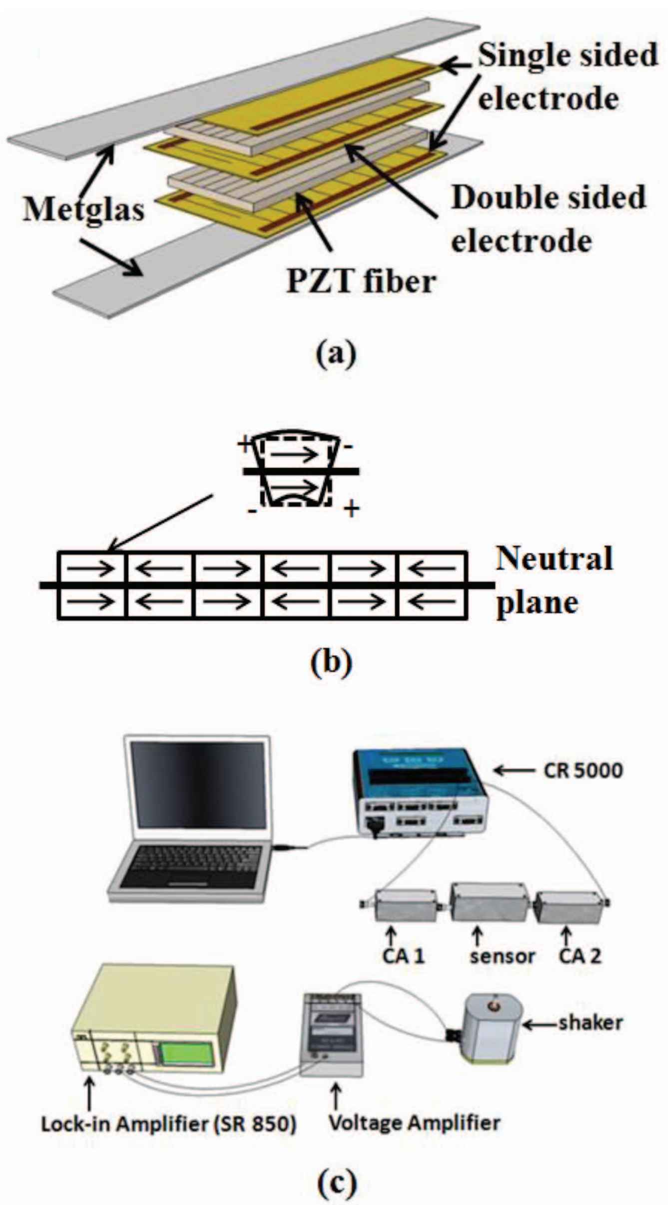

Fig. 1. (a) Schematic of our new differential mode ME laminate sensor; (b) poling profile of multi-push/pull, dual-PZT composite structure; and (c) schematic of the experimental signal path.

A schematic of the experimental setup for the evaluation of the differential mode structure of the Metglas/PZT laminates is shown in Fig. 1(c). Information about the relative amplitude of and the phase shift between signals from the top and bottom PZT layer is important to understanding the different deformation modes excited by an applied magnetic signal relative to those excited by an applied vibrational signal. To analyze the signal from each PZT layer individually, the charge generated by each PZT layer was converted to a voltage, via integration using custom-built charge amplifier circuits (CA1, CA2) [13]. The raw voltage signals were recorded using a datalogger (CR5000, Campbell Scientific Inc., Logan, UT) and uploaded to a PC for analysis using MATLAB (The MathWorks, Natick, MA). Vibrational signals were generated using an LDS V203 10/32 shaker (Brüel and Kjær AS, Nærum, Denmark). The shaker was driven by a 10-Hz sinusoidal output signal from an SR850 lock-in amplifier (Stanford Research Systems Inc., Sunnyvale, CA) augmented by an LDS PA25E power amplifier (Brüel and Kjær AS). Magnetic test fields of frequency 10 Hz were generated using the output of the lock-in amplifier, and then fed into a custom-built 100-turn Helmholtz coil with a 45 mm radius.

To compare the two signals generated by each sensor, the charge outputs were converted into equivalent magnetic signals using a calibration factor. The magnetoelectric charge coefficient (α_{MEQ}) was measured for each sensor by exposing the sensor to a calibrated dc magnetic field of around 10 Oe to get the maximum ME coefficient, which is around 20 V/cm·Oe in this test. The ME coefficient for each sensor, coupled with the gain factor of the charge amplifier, allows a calibration factor to be calculated for each sensor:

$$\text{Calibration factor}\left[\frac{\mathrm{T}}{\mathrm{V}}\right] = \frac{1}{\alpha_{\mathrm{ME}}\left[\frac{\mathrm{pC}}{10^{-4}\mathrm{T}}\right]\text{C.A. gain factor}\left[\frac{\mathrm{V}}{\mathrm{pC}}\right]}. \tag{1}$$

III. Results and Discussions

First, the response of the sensors to an induced vibrational signal was measured and analyzed. Using the

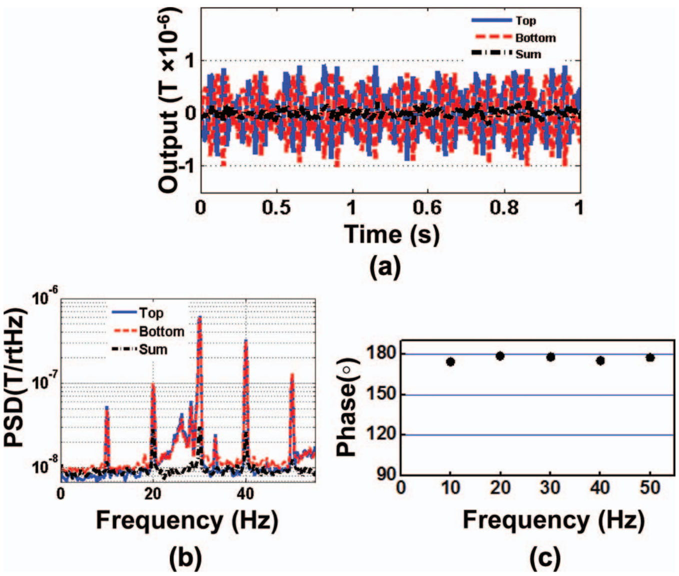

Fig. 2. (a) Time-domain equivalent magnetic response of differential mode sensor to incident vibrational signal; (b) power spectral density of top, bottom, and time-domain summation of top and bottom; and (c) phase shift between top and bottom PZT layers as a function of frequency calculated from a linear time-invariant transfer function.

calibration factor given previously, the equivalent ac magnetic signal was calculated from the output voltage of each charge amplifier.

The response of each layer of the differential sensor, as well as the summation of the constituent signals, is presented in Fig. 2(a). In this figure, the solid line shows the output signal from the top PZT layer, the dashed line is the signal generated by the bottom PZT layer, and the dot-dashed line is the time-domain summation of the top and bottom PZT layers. Fig. 2(a) shows that the amplitude of the combined signal (dot-dashed trace) is significantly attenuated relative to either of the two constituent output signals (dashed and solid traces). To more accurately analyze the data, the power spectral density (PSD) of each component signal and of the time-domain summation of the two signals was calculated using MATLAB. Additionally, a linear, time-invariant transfer function between the constituent output signals was estimated using built-in MATLAB commands. The phase shift between the top and bottom PZT layers as a function of frequency can then be calculated from the estimated transfer function.

Fig. 2(b) shows the power density of the output signals of the top, bottom, and time-domain summation over the frequency range from dc to 55 Hz. At the vibrational drive frequency of 10 Hz, the amplitude of the summation signal was 5 times smaller than either that of the top or bottom PZT layers (10^{-8} T/$\sqrt{\text{Hz}}$ versus 5 $\times$ 10^{-8} T/$\sqrt{\text{Hz}}$, respectively). In addition, the second-, third-, fourth-, and fifth-harmonic signals (20, 30, 40, and 50 Hz) exhibited the same trends. The summation signal of the third harmonic was 10-fold attenuated. In fact, the differential structure ME sensor also shows the significant

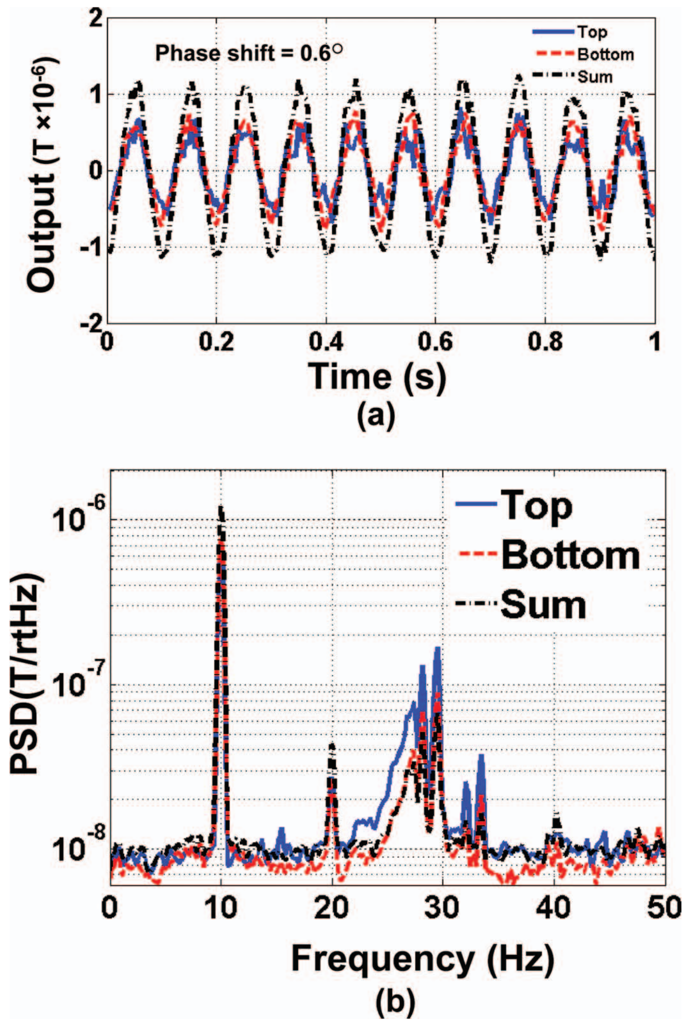

Fig. 3. (a) Time-domain response of top PZT layer, bottom, and sum of individual signals in response to an incident magnetic field; and (b) power spectral density response of a sensor to a 10 Hz magnetic field.

cancellation to the vibrational noise at frequency range from 10 Hz to hundreds of hertz.

Fig. 2(c) shows the calculated phase shift between the output signals as function of frequency upon exposing the differential ME structure to a 10 Hz vibrational signal. At 10 Hz, as well as at the higher-order harmonics, the phase shift between the top and bottom PZT layers was quite close to 180°. This phase shift data supports our hypothesis that vibrational signals tend to excite the differential ME structure in a bending mode deformation, in which the top and bottom layers are phase shifted, enabling cancellation of that vibrational signal in summation.

To examine the response of the sensor to an incident magnetic field, the shaker was replaced by a 90-mm, 100-turn Helmholtz coil driven at a frequency of 10 Hz by an SR850 lock-in amplifier. Fig. 3(a) shows the time domain response of the sensor to an incident 10 Hz magnetic field. The signals from the top and bottom PZT layers are nearly in-phase, resulting in an approximate doubling of the output signal upon summation. The relative phase shift between the top and bottom PZT layers at 10 Hz was only

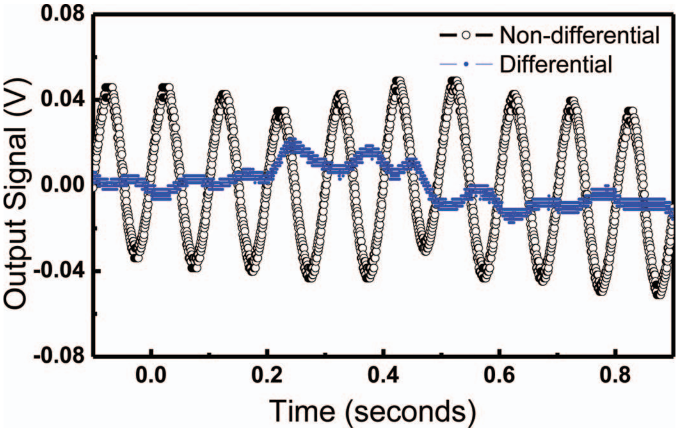

Fig. 4. Comparison of noise cancellation for a differential ME structure sensor and a non-differential ME structure sensor.

0.6°, which indicates that incident magnetic fields result in a longitudinal-mode deformation of the differential ME structure.

The power spectral density response to the 10 Hz magnetic field over the range of dc to 55 Hz is shown in Fig. 3(b). Characteristic of the ME laminate sensor's magnetic response, the 10 Hz first-harmonic signal was dominant relative to the higher-harmonic signals (20 Hz, 30 Hz, etc.). The power spectral density of the summation signal was doubled in amplitude relative to the individual component layers at 10 Hz (1.4 $\mu T/\sqrt{Hz}$ versus 0.7 $\mu T/\sqrt{Hz}$, respectively).

Finally, the capability for vibrational signal cancellation of our new differential ME structure was compared with that of a non-differential one of similar geometry. Following analysis similar to that given previously, the different working modes under various excitation sources were studied. The results demonstrate that the new differential structure has the ability to reject an incident vibrational signal by summation of the signals of the top and bottom PZT layers. In this measurement, the top and bottom PZT layers were connected in parallel at first, and a single charge amplifier was used to collect the signal. Simultaneously, a second, non-differential ME laminate connected to another charge amplifier was used as a control group. Both signals were observed together using an oscilloscope. The shaker was put in the middle of the differential and non-differential ME structures and a 10 Hz driving signal was excited.

Fig. 4 shows the signals from the differential and non-differential ME sensors, obtained directly from the oscilloscope. In this figure, the signal amplitude of the non-differential sensor was about 80 mV, whereas that of the differential ME structure was only about 20 mV. Clearly, our new differential structure shows excellent ability to cancel vibrational signals. Furthermore, the fact that we can separate magnetic and vibrational signals is important, in and of itself. Hybrid sensors capable of data fusion between two separated signals of an environment could be enabled.

IV. Summary

In summary, we present a novel structure for Metglas/PZT-based ME laminate sensors that has excellent capacity for vibrational signal cancellation without reduction of the magnetic signal response. The ability of the structure to attenuate vibrational signals by 10 to 20 dB may allow for practical applications of such sensors in real-world environments in which contamination of magnetic signals by external vibrational noise increases the equivalent magnetic noise floor.

References

[1] M. I. Bichurin, V. M. Petrov, and G. Srinivasan, "Resonance magnetoelectric effects in layered magnetostrictive-piezoelectric composites," *Phys. Rev. B*, vol. 68, no. 13, art. no. 054402, 2003.

[2] M. Fiebig, "Revival of the magnetoelectric effect," *J. Phys. D*, vol. 38, no. 8, pp. R123–R152, 2005.

[3] G. T. Rado and V. J. Folen, "Observation of the magnetically induced magnetoelectric effect and evidence for antiferromagnetic domains," *Phys. Rev. Lett.*, vol. 7, no. 8, pp. 310–311, 1961.

[4] J. Das, Y. Song, N. Mo, P. Krivosik, and C. E. Patton, "Electric-field-tunable low loss multiferroic ferrimagnetic-ferroelectric heterostructures," *Adv. Mater. (Deerfield Beach Fla.)*, vol. 21, no. 20, pp. 2045–2049, 2009.

[5] S. X. Dong, J. Y. Zhai, F. M. Bai, J. F. Li, D. Viehland, and T. A. Lograsso, "Fe–Ga/Pb($Mg_{1/3}Nb_{2/3}$)O_3–$PbTiO_3$ magnetoelectric laminate composites," *J. Appl. Phys.*, vol. 97, no. 22, art. no. 103902, 2005.

[6] Z. P. Xing, S. X. Dong, J. Y. Zhai, L. Yan, J. F. Li, and D. Viehland, "Resonant bending mode of Terfenol-D/steel/Pb(Zr,Ti)O_3 magnetoelectric laminate composites," *Appl. Phys. Lett.*, vol. 89, no. 11, art. no. 112911, 2006.

[7] C.-W. Nan, M. I. Bichurin, S. Dong, D. Viehland, and G. Srinivasan, "Multiferroic magnetoelectric composites: Historical perspective, status, and future directions," *J. Appl. Phys.*, vol. 103, no. 3, art. no. 031101, 2008.

[8] J. Zhai, Z. Xing, S. X. Dong, J. F. Li, and D. Viehland, "Magnetoelectric laminate composites: An overview," *J. Am. Ceram. Soc.*, vol. 91, no. 2, pp. 351–358, 2008.

[9] S. X. Dong, J. Y. Zhai, J.-F. Li, and D. Viehland, "Magnetoelectric effect in Terfenol-D/Pb(Zr,Ti$O)_3$/μ-metal laminate composites," *Appl. Phys. Lett.*, vol. 89, no. 12, art. no. 252904, 2006.

[10] J. Y. Zhai, Z. P. Xing, S. X. Dong, J. F. Li, and D. Viehland, "Thermal noise cancellation in symmetric magnetoelectric bimorph laminates," *Appl. Phys. Lett.*, vol. 93, no. 7, art. no. 072906, 2008.

[11] Z. P. Xing, J. Y. Zhai, J. F. Li, and D. Viehland, "Investigation of external noise and its rejection in magnetoelectric sensor design," *J. Appl. Phys.*, vol. 106, no. 2, art. no. 024512, 2009.

[12] J. Das, J. Gao, Z. Xing, J. F. Li, and D. Viehland, "Enhancement in the field sensitivity of magnetoelectric laminate heterostructures," *Appl. Phys. Lett.*, vol. 95, no. 9, art. no. 092501, 2009.

[13] Z. P. Xing, J. Y. Zhai, S. X. Dong, J. F. Li, D. Viehland, and W. G. Odendaal, "Modeling and detection of quasi-static nanotesla magnetic field variations using magnetoelectric laminate sensors," *Meas. Sci. Technol.*, vol. 19, no. 1, art. no. 015206, 2008.

Authors' photographs and biographies were unavailable at time of publication.